Journal of Applied Microbiology, 2024, 135, 1–11
https://doi.org/10.1093/jambio/lxad313
Advance access publication date: 20 December 2023
Research Article

JOURNAL OF APPLIED MICROBIOLOGY
OXFORD UNIVERSITY PRESS

Exploring the potential of the halotolerant bacterial strain *Bacillus subtilis* LN8B as an ecofriendly sulfide collector for seawater flotation

Dayana Arias [1,*], Manuel Saldaña[2], Yesica L. Botero[3], Francisco Dinamarca[4], Bernardo Paredes[4], Camila Salazar-Ardiles[1], David C. Andrade[5], Luis A. Cisternas[3], Jorge Carrasco[6], Carlos Santos[6], Cristina Dorador[7], Benito Gómez-Silva[4]

[1]Laboratory of Molecular Biology and Applied Microbiology, Research Center in High Altitude Medicine and Physiology, Biomedical Department, Faculty of Health Science, Universidad de Antofagasta, Av. Angamos 601, Antofagasta 1270300, Chile
[2]Faculty of Engineering and Architecture, Arturo Prat University, Iquique 1110939, Chile
[3]Departamento de Ingeniería Química y Procesos de Minerales, Universidad de Antofagasta, Av. Angamos 601, Antofagasta 1270300, Chile
[4]Biochemistry Lab., Biomedical Dept., Health Sciences Faculty and Centre for Biotechnology and Bioengineering (CeBiB), Universidad de Antofagasta, Av. Angamos 601, Antofagasta 1270300, Chile
[5]Exercise Applied Physiology Laboratory, Research Center in High Altitude Medicine and Physiology, Biomedical Department, Faculty of Health Science, Universidad de Antofagasta, Av. Angamos 601, Antofagasta 1270300, Chile
[6]Departamento de Ingeniería en Minas, Facultad de Ingeniería, Universidad de Antofagasta, Av. Angamos 601, Antofagasta 1270300, Chile
[7]Department of Biotechnology, Faculty of Marine Sciences and Biological Resources and Centre for Biotechnology and Bioengineering (CeBiB), Universidad de Antofagasta, Av. Angamos 601, Antofagasta 1270300, Chile

*Corresponding author. Av. Angamos 601, Antofagasta 1270300, Chile. E-mail: dayana.arias.t@gmail.com; dayana.arias@uantof.cl

Abstract

Aim: To assess the effectiveness of *Bacillus subtilis* strain LN8B as a biocollector for recovering pyrite (Py) and chalcopyrite (CPy) in both seawater (Sw) and deionized water (Dw), and to explore the underlying adhesion mechanism in these bioflotation experiments.

Materials and Methods: The bioflotation test utilized *B. subtilis* strain LN8B as the biocollector through microflotation experiments. Additionally, frother methyl isobutyl carbinol (MIBC) and conventional collector potassium amyl xanthate (PAX) were introduced in some experiments. The zeta potential (ZP) and Fourier-transform infrared spectroscopy (FTIR) was employed to explore the adhesion mechanism of Py and CPy interacting with the biocollector in Sw and Dw. The adaptability of the *B. subtilis* strain to different water types and salinities was assessed through growth curves measuring optical density. Finally, antibiotic susceptibility tests were conducted to evaluate potential risks of the biocollector.

Results: Superior outcomes were observed in Sw where Py and CPy recovery was ~39.3% ± 7.7% and 41.1% ± 5.8%, respectively, without microorganisms' presence. However, *B. subtilis* LN8B potentiate Py and CPy recovery, reaching 72.8% ± 4.9% and 84.6% ± 1.5%, respectively. When MIBC was added, only the Py recovery was improved (89.4% ± 3.6%), depicting an adverse effect for CPy (81.8% ± 1.1%). ZP measurements indicated increased mineral surface hydrophobicity when Py and CPy interacted with the biocollector in both Sw and Dw. FTIR revealed the presence of protein-related amide peaks, highlighting the hydrophobic nature of the bacterium. The adaptability of this strain to diverse water types and salinities was assessed, demonstrating remarkable growth versatility. Antibiotic susceptibility tests indicated that *B. subtilis* LN8B was susceptible to 23 of the 25 antibiotics examined, suggesting it poses minimal environmental risks.

Conclusions: The study substantiates the biotechnological promise of *B. subtilis* strain LN8B as an efficient sulfide collector for promoting cleaner mineral production. This effectiveness is attributed to its ability to induce mineral surface hydrophobicity, a result of the distinct characteristics of proteins within its cell wall.

Impact Statement

The findings of this research hold promising implications for the utilization of bioflotation in advancing ecofriendly mineral recovery processes, emphasizing a notable step toward the adoption of more environmentally conscious mining practices.

Keywords: *Bacillus subtilis*, pyrite, chalcopyrite, collectors, depressants, flotation, bioflotation

Introduction

Porphyry copper ores are mineralogically composed of copper sulfide minerals such as chalcopyrite (CPy), covellite, chalcocite and other sulfides such as pyrite (Py) and arsenopyrite. CPy and Py are the highest-grade sulfide minerals in these ores. CPy serves as a copper source, while Py is the sulfide gangue mineral traditionally separated from copper sulfides. Froth flotation is the standard method for selectively separating CPy from Py (Elshkaki et al. 2016).

Froth flotation hinges upon the intrinsic surface characteristics of minerals, instigating the buoyancy or disposition of one or multiple minerals into the tailings. These surface attributes of minerals can be purposefully tailored using a suite of reagents, encompassing collecting reagents, depressants, foaming agents, and modifiers. Collectors undergo adsorption

Received 20 November 2023; **revised** 12 December 2023; **accepted** 19 December 2023
© The Author(s) 2023. Published by Oxford University Press on behalf of Applied Microbiology International. All rights reserved. For permissions, please e-mail: journals.permissions@oup.com

Downloaded from https://academic.oup.com/jambio/article/135/1/lxad313/7485925 by Universidad de Antofagasta user on 26 January 2026

onto mineral surfaces, bestowing hydrophobic traits upon the target particles and facilitating their flotation. Depressants cause the opposite effect, i.e. to prevent the collection of other unwanted mineral species in the concentrate. Foaming agents, which act as surfactants, shape the surface properties of bubbles, mitigating their tendency to coalesce. Meanwhile, modifiers function as reagents that fine-tune the collectors' performance by augmenting their selectivity, thereby regulating the flotation conditions (Oulkhir et al. 2023).

The traditional way to conduct the flotation process is to depress the Py in the first stage of the flotation. Then, the tailings produced end up with acidifying species, which likely produced acid mine drainage (AMD), a substantial environmental concern (Benzaazoua et al. 2000, 2017, Nadeif et al. 2019, Skandrani et al. 2019). Therefore, framed in the concept of cleaner production, an alternative procedure to prevent AMD from tailings is the desulfurization process, which aims to float all the sulfide minerals (e.g. copper sulfides and Py) in an early stage of the flotation process and produce a tailing with low content of sulfide species. Therefore, desulfurization seems to be a promising approach for AMD prevention (Ait-Khouia et al. 2021). Nevertheless, some issues are related to selecting the reagents to be used during the flotation process. For instance, the choice of the collectors. Traditional collectors used in flotation process are xanthate, which is toxic, and they aggravate the final state of tailings since the xanthate collector decomposes in water or an aqueous solution, producing carbon disulfide (CS_2), the latter is a flammable and toxic gas (Shen et al. 2016).

Another concern associated with the flotation process is the use of water. The flotation process requires considerable water input to obtain the concentrate (Cisternas and Gálvez 2018). Nowadays, more copper mining companies worldwide are facing water scarcity. The outlook for the freshwater available to carry out mining operations is uncertain, and it is getting worse over the years due to climate change, where periods of drought are increasingly latent (Jeldres et al. 2016). According to this, some copper mining companies use seawater (Sw) to conduct flotation (Cisternas and Gálvez 2018). For instance, Chile has some copper mining operations using Sw, most of them are in northern Chile, where freshwater sources have been overexploited over the years (Rao et al. 2017). The use of Sw is beneficial for the flotation process. For instance, the frothing in saline water is much more efficient than in fresh water. This is because in saline water, the inorganic electrolytes, such as NaCl, KCl, $MgCl_2$, $CaCl_2$, and Na_2SO_4, can inhibit bubble coalescence and stabilize the froth layer. Also, adding frothers produces finer bubbles and a lower amount of frother is required to conduct the procedure (Castro et al. 2013, Suyantara et al. 2018, Arancibia-Bravo et al. 2019). The frothing plays an essential role in the flotation process since the hydrophobic valuable minerals are attached to air bubbles in the froth, which enables the recovery of particles in the concentrate (Wills and Napier-Munn 2016). Nevertheless, Sw has a complex composition; therefore, the presence of some species can affect the floatability of sulfide minerals. For instance, the presence of divalent Mg^{2+} ions render hydrophilic the surface of sulfide minerals, decreasing the performance of traditional collectors as the xanthates (Li et al. 2019).

Hence, recognizing the imperative to explore ecofriendly alternatives for xanthate collectors that can function effectively in Sw conditions, the emergence of microbial-origin collectors, or biocollectors, aligns with the concept of bioflotation. Bioflotation is based on the premise that bacteria and/or their metabolic products (proteins and extracellular polysaccharides) interact naturally with different minerals, modifying the surface properties such as zeta potentials and hydrophobicity (Aksoy et al. 2022, Arias et al. 2023). Various mechanisms by which microorganisms interact with mineral surfaces have been postulated. These interactions induce significant alterations in surface characteristics, including (i) the adherence of bacterial cells to mineral surfaces, effectively shaping the mineral characteristics based on microbial attributes, (ii) oxidation or reduction reactions, and (iii) adsorption and chemical reactions involving metabolic byproducts (Rao et al. 2010, Dwyer et al. 2012, House and Rilski).

In this work, the halotolerant bacterial strain *Bacillus subtilis* LN8B, previously isolated from Laguna Salada in the Atacama Desert, was used as a biocollector for CPy and Py environmental desulfurization (Arias et al. 2019). Halophiles and halotolerant species can live in high-salinity conditions such as hypersaline lakes, coastal dunes, saline deserts, inland salt seas, and springs (Martínez et al. 2022). The trend toward harnessing halophiles and halotolerant species to create a cost-effective biotreatment infrastructure is gaining momentum. This approach offers a range of advantages, including reduced energy consumption, diminished need for freshwater, minimized initial capital outlay, and the potential for uninterrupted production especially for their use in flotation processes in regions like Chile, where Sw can be used directly to grow bacteria (Yin et al. 2015). On the other hand, halophilic bacteria tend to be more biodegradable and, in some instances, could provide highly selective flotation schemes.

Thus, the general objective was to compare the performance of this alternative collector to the performance of the xanthate's collectors. Also, to understand the adsorption mechanisms between the biocollector and minerals surfaces. Implementing these two strategies, desulfurization and using biocollectors enables mine operations to be more sustainable and respectful of the environment. The physicochemical interaction between Sw and freshwater (as deionized water, Dw) with the biocollector obtained from the halotolerant bacterial strain *Bacillus subtilis* LN8B is unknown. Therefore, this work aims to study the effect of the type of water in the growth conditions of the biocollector, the adsorption of the biocollector on CPy and Py surfaces, to assess if this biocollector can be used to float both CPy and Py during the desulfurization process. Finally, the adsorption mechanisms of the system biocollector-Sw/fresh water-mineral surface will be assessed using zeta potential and Fourier-transform infrared spectroscopy (FTIR).

Materials and methods

Effect of the type of water and salinities on the bacterial growth

Bacillus subtilis LN8B was previously isolated from Laguna Salada in the Atacama Desert according to Arias et al. (2019). To assess the influence of water type and salinity on bacterial growth, cells were cultured in 100 ml volumes in 250 ml Erlenmeyer flasks at 30°C. The culture medium consisted of peptone (PE) at 10 g l^{-1} and yeast extract (YE) at 5 g l^{-1}, dissolved in (i) Sw, (ii) Dw, and (iii) Dw supplemented with 2.5%, 5.0%, 7.5%, and 10.0% NaCl. Once the salinity was evaluated and the best growth was selected and its cultivation was assessed at the following temperatures: 4°C, 25°C,

Downloaded from https://academic.oup.com/jambio/article/135/1/lxad313/7485925 by Universidad de Antofagasta user on 26 January 2026

Table 1. Quantitative analysis (%) of minerals used in the study.

Crystalline phase	Py, abundance %	CPy, abundance %
Pyrite, FeS_2	Majority	–
Chalcopyrite, $CuFeS_2$	19.5	80.5

Table 2. Sw ion concentration and method of analysis.

Parameter	Concentration	Method of analysis
Na^+ (mg l^{-1})	11 140 ± 41	Atomic absorption
Ca^{2+} (mg l^{-1})	400 ± 15	Atomic absorption
Mg^{2+} (mg l^{-1})	1269 ± 38	Atomic absorption
K^+ (mg l^{-1})	398 ± 19	Atomic absorption
Cl^- (mg l^{-1})	20 971 ± 55	Argentometric method
HCO_3^- (mg l^{-1})	120 ± 15	Acid–base titration
pH	7.97 ± 0.6	Multiparameter

30°C, 37°C, 45°C, and 60°C. Growth was assessed by monitoring absorbance changes at 600 nm with a JASCO V-700 spectrophotometer (Jasco Corp, Tokyo, Japan). The doubling time was computed during the exponential phase and subsequently documented and organized into a table.

Antibiotic susceptibility

Overnight-cultured cells in medium containing PE, YE, and 2.5% NaCl at 30°C were diluted with a sterile saline solution according to McFarland scale N○ 5. The diluted cells were spread as a layer on Mueller–Hinton (MH) (BD Difco™) agar plates for antibiotic susceptibility testing. The disc diffusion method was employed, using 25 different antibiotics at specific concentrations, including oxolinic acid (2 μg), lincomycin (2 μg), amox. clavulanic acid (20/10 μg), amoxicillin (25 μg), linezolid (30 μg), fosfomycin (200 μg), amoxicillin sulbactam (10/10 μg), meropenem (10 μg), ertapenem (10 μg), oxacillin (1 μg), tetracycline (30 μg), streptomycin HLRA (300 μg), clindamycin (2 μg), imipenem (10 μg), cefotaxime (30 μg), amikacin (30 μg), cefepime (30 μg), sulfatrimetoprim (25 μg), ciprofloxacin (5 μg), cefadroxil (30 μg), gentamicin (10 μg), ampicillin/sulbactam (10 μg), ampicillin (10 μg), vancomycin (30 μg), and gentamicin 120 (120 μg). The discs were placed on the agar, left to dry for 10–15 min, and then incubated at 37°C for 18–24 h. The diameters of the inhibition zones were measured and compared to the data table from Emarin Sda S.A., Ñuñoa, Santiago, Chile (https://www.emarinsda.com).

Mineral and Sw characterization

CPy ($CuFeS_2$) and Py (FeS_2) minerals used in this study were purchased from Ward's Science (Rochester, NY, USA). The minerals were initially crushed and ground by hand (to manually sorted gangue mineral), in an agate mortar until reaching a particle size of ∼600 μm. Then, the minerals with this particle size were further ground in an automatic agate mortar to get the particle size −74 + 43 μm, required to run the bioflotation experiments. It is worth mentioning that the ground in the automatic agate mortar was conducted immediately before running the bioflotation to avoid mineral surface oxidation. Finally, a representative sample of each mineral was analyzed by X-ray diffraction to corroborate the final purity (Table 1).

The water samples used were Dw and Sw. Sw was collected from San Jorge Bay in Antofagasta, Chile (−23.703672, −70.425199) and filtered with the following sequence of pore size to remove microorganisms before use: 10, 5, 1, and 0.22 μm. Physicochemical characterization of Sw was performed in triplicate and the ion concentration and method of analysis are represented in Table 2. The measurements of pH, temperature, dissolved oxygen (DO), and conductivity were performed by the multiparameter probe (HI98194 Multiparameter, Hanna Instruments, USA).

Bioflotation tests

The biocollector for bioflotation tests was cultured in the laboratory using PE and YE supplemented with Sw and Dw. After 24 h of incubation on a rotary shaker at 30°C, the cultures were centrifuged and washed with sterilized water for further experiments. Bioflotation tests were performed through microflotation experiments using a modified Hallimond-type flotation cell as described in Botero et al. (2022) with the following modifications: For experiments with the biocollector, metabolite-free cells were dissolved in sterilized water (Dw or Sw) and mixed with 1 g of mineral. The final cell concentration used for each microflotation was 1×10^9 cells ml^{-1}. These values were determined through cell counting using a Neubauer-improved glass counting chamber (Marienfeld, Germany) with a depth of 0.01 mm. The original culture was then diluted to the desired concentration in a total volume of 150 ml, corresponding to the volume of the microflotation cell. After that, the mineral was conditioned for 15 min at 200 rpm and transferred to the Hallimond tube for the bioflotation. For the experiments with frother, 10 ppm of methyl isobutyl carbinol (MIBC) were added and for experiments with conventional collector, 50 ppm potassium amyl xanthate (PAX) were used and conditioned for the same period. The bioflotations conditions for all the experiments were an airflow rate of 20 ml min^{-1}, magnetic stirring between 800 and 1000 rpm, and flotation time of 5 min. The pulp level was kept constant by adding a background solution (Sw or Dw at the desired pH). All bioflotation tests were performed in triplicate, and their respective standard deviations are provided in the text. Subsequently, the nonfloated and floated products were dried and weighed to determine the mineral floatability.

Adsorption test

Adsorption tests were carried out to study the chemical interaction in the two types of water between the mineral surface and the biocollector. Zeta potential measurements were performed on a Zeta Meter System 3.0 + microelectrophoresis apparatus. The mineral size was ≤10 μm at concentration of 0.05% by weight, and the biomass suspension of 1×10^9 cells ml^{-1}. The experiments were performed in Sw and Dw; for both, pHs evaluated were 2, 4, 6, 8, and 10. In the case of Dw, 0.01 M NaCl was used as the indifferent electrolyte. The conditions at each pH were the following: (i) biocollector, (ii) Py, (iii) CPy, (iv) Py-biocollector, and (v) CPy-biocollector. For spectroscopic studies, FTIR (Perkin Elmer) operated in the range of in the range of 4000 to 400 cm^{-1} was used. For this, 0.1 g of the fine fraction (particle size of ≤10 μm) of mineral (Py or CPy) was added in 10 ml of water (Sw or Dw), mixed with the biocollector at a final concentration of 1×10^9 cells ml^{-1} and stirring for 15 min at 200 rpm. After that, the mineral slurry was washed with the corresponding type of water,

Downloaded from https://academic.oup.com/jambio/article/135/1/lxad313/7485925 by Universidad de Antofagasta user on 26 January 2026

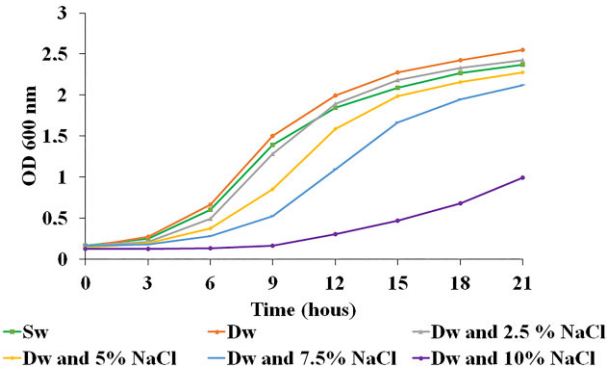


Figure 1. Growth curves of *B. subtilis* LN8B cultured with Dw, Sw, and different concentrations of NaCl and 30°C of temperature.

filtered, and dried at 37°C. The filters were scraped, and the powder was analyzed by FTIR. To analyze the spectroscopic pattern of the bio-collector, the bacterial cells were washed and lyophilized before measurements.

Results

Effect of the type of water and salinities on *B. subtilis* LN8B growth

Figure 1 and Table 3 summarize the growth curves and doubling times after *B. subtilis* LN8B was grown at 30°C in Sw or Dw supplemented with different NaCl concentrations. Similar doubling times (2.4 h) were obtained when the bacterium was grown in media prepared in Sw or Dw in the absence of added salt. A lower doubling time (2.3 h) was achieved when growth was conducted at a final 2.5% NaCl; however, higher salinities substantially increased doubling times. The shortest doubling time at 2.5% NaCl was only observed at 30°C, while experiencing low or no growth at 0°C, 45°C, or 60°C (data not shown). Then, *B. subtilis* LN8B exhibits characteristics indicative of a mesophilic, halotolerant microorganism, demonstrating efficient growth in both Sw and Dw supplemented with 2.5% NaCl, particularly at a temperature of 30°C.

Antibiotic susceptibility of the biocollector

Since resistance/susceptibility to antibiotics is significant for using microorganisms in industrial processes, the growth of strain *B. subtilis* LN8B was challenged with 25 antibiotics and evaluated by the disc–diffusion test in cells cultured in MH agar plates (Table 4). Remarkably, based on the inhibitory zone diameters, the biocollector was resistant to two antibiotics, fosfomycin and cefepime.

Bioflotation tests

Bioflotation experiments were carried out to evaluate the performance of the biocollector on the flotability of Py and CPy using Sw and Dw in the first instance (Fig. 2). In the case of Py with Sw (Fig. 2a) at natural pH (pH 8), the recovery of the mineral using only the biocollector (Py+, F−, B+, C−) yielded a recovery of 72.8% ± 4.9%, much greater than the recovery obtained by the natural buoyancy of the Py, which was 39.3% ± 7.7%. When evaluating the action of the biocollector at the same pH 8 (Py+, F−, B+, C) in Dw, the buoyancy was 58.4% ± 7.8% compared to the control of the natural buoyancy of Py in Dw, (Py+, F−, B−, C−) with a recovery of 43% ± 4.2%. In the case of CPy in Sw (Fig. 2b), the recovery of the mineral by the action of the biocollector (CPy+, F−, B+, C−) was 84.6% ± 1.5%. Comparing this behavior with their respective control, it is evident that the biocollector increases the recovery since the natural buoyancy of the mineral (CPy+, F−, B−, C−) was 41.1% ± 5.8%.

When bioflotation experiments were performed with Dw and the biocollector (CPy+, F−, B+, C−), mineral recovery was 74.5% ± 2.9%, while the recovery under the control condition (CPy+, F−, B−, C−) was 43.8% ± 3.3%. These antecedents indicate that the sulfide biocollector performs better in Sw than in Dw for both sulfide minerals.

Because a better recovery was observed when Sw was utilized, experiments to undertand the behavior of the biocollector with other components of the process were carried out by adding collector PAX and MIBC as frother (Fig. 3). In the case of Py, the addition MIBC to the action of the bio collector (Py+, F+, B+, C−) increases the recovery up to 89.4% ±

Table 4. Susceptibility of the biocollector to 25 antibiotics.

Antibiotic	Potency (μg)	Inhibition zone (mm)
Oxolinic acid	2	S(0)
Lincomycin	2	S(46)
Amox. clavulanic acid	20/10	S(40)
Amoxicillin	25	S(46)
Linezolid	30	S(44)
Fosfomycin	200	R(14)
Amox. sulbactam	10/10	S(42)
Meropenem	10	S(40)
Ertapenem	10	S(38)
Oxacillin	1	S(0)
Tetracycline	30	S(30)
Streptomycin hlar	300	S(32)
Clindamycin	2	S(34)
Imipenem	10	S(36)
Cefotaxime	30	S(36)
Amikacin	30	S(0)
Cefepime	30	R(16)
Sulfatrimetoprim	25	S(34)
Ciprofloxacin	5	S(26)
Cefadroxil	30	S(40)
Gentamicin	10	S(34)
Ampicillin/sulbactam	10	S(24)
Ampicillin	10	S(28)
Vancomycin	30	S(28)
Gentamicin 120	120	S(44)

Cells were grown in MH agar plates and incubated at 37°C for 18–24 h in the presence of disc-containing antibiotics. The diameter of the inhibition zones and their interpretation were done according to the manufacturer's instruction (SDA). R: resistant; S: susceptible. Numbers in parentheses represent the diameters of the inhibition halos in millimeters.

Table 3. Doubling time for strain *B. subtilis* LN8B grown in Sw or Dw without or added NaCl.

	Sw		Dw			
NaCl (%)	None	0	2.5	5	7.5	10
Doubling time (h)	2.42 ± 0.002	2.41 ± 0.001	2.28 ± 0.001	2.89 ± 0.002	3.42 ± 0.001	4.71 ± 0.001

Downloaded from https://academic.oup.com/jambio/article/135/1/lxad313/7485925 by Universidad de Antofagasta user on 26 January 2026

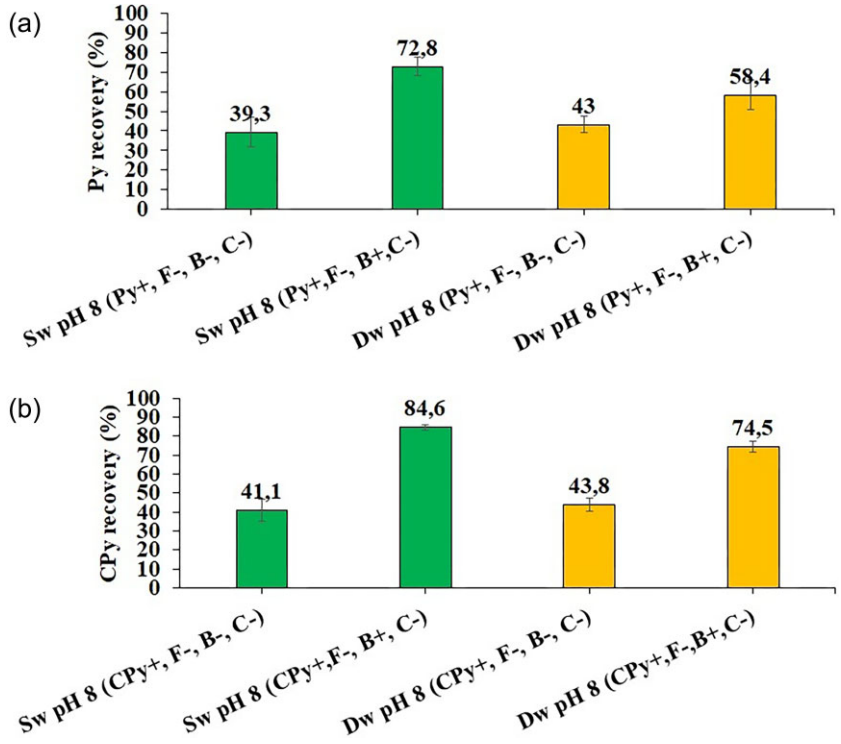


Figure 2. Bioflotation experiments using the biocollector in Sw (green) and Dw (yellow) for Py (a) and CPy (b), respectively. B represents the biocollector, C the collector PAX, and F the frother MIBC. The signs + and − indicate the presence or absence in the experiments.

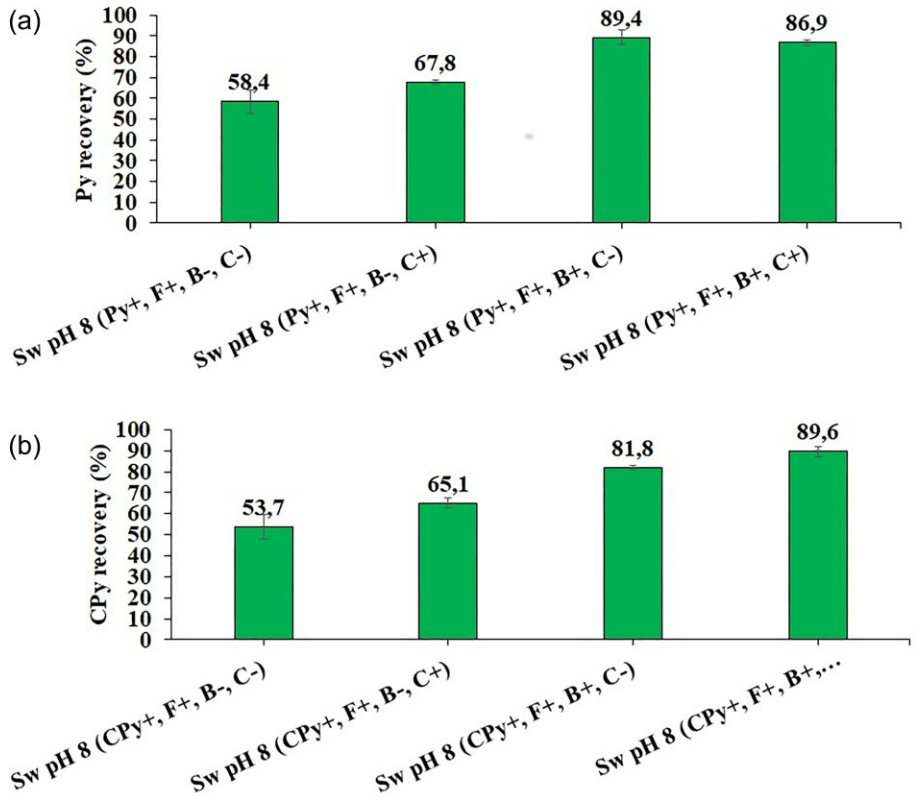


Figure 3. Bioflotation experiments the biocollector in Sw for Py (a) and CPy (b), respectively. B represents the biocollector, C the collector PAX, and F the frother MIBC. The signs + and − indicate the presence or absence in the experiments.

Downloaded from https://academic.oup.com/jambio/article/135/1/lxad313/7485925 by Universidad de Antofagasta user on 26 January 2026

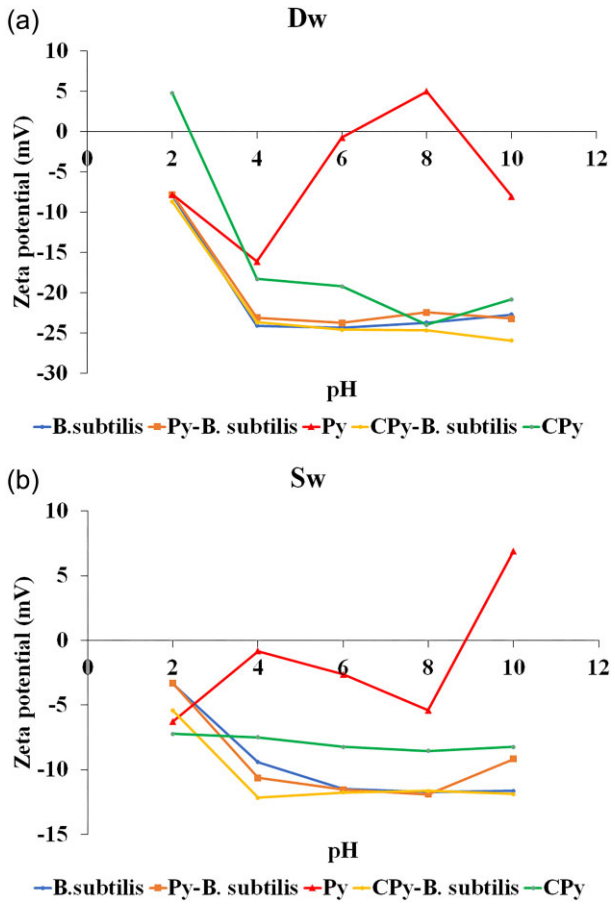


Figure 4. Zeta potential of Py and CPy before and after treatment with the biocollector at natural pH in Dw (a) and Sw (b).

3.6% compared to the control of the mineral Py and MIBC (Py+, F+, B−, C−), which as a recovery of 58.4% ± 5.5%, and control of the Py, MIBC, and PAX (Py+, F+, B−, C+), which as a recovery of 67.8% ± 1.2%. Finally, to evaluate if the biocollector enhances the Py recovery when the traditional PAX collector is used, bioflotation experiments were performed by adding all the reagents together with the biocollector (Py+, F+, B+, C+) obtaining a recovery of the 86.9% ± 1.5%. In the case of CPy, the addition of MIBC and the biocollector (CPy+, F+, B+, C−) increases the recovery up to 81.8% ± 1.1% compared to the control of the mineral CPy and MIBC (CPy+, F+, B−, C−), which as a recovery of 53.7% ± 5.9%, and control of the CPy, MIBC, and PAX (Py+, F+, B−, C+), which as a recovery of 65.1% ± 2.3%. The experiments destined to evaluate the enhancement of the biocollector in conventional bioflotation (CPy+, F+, B+, C+) indicate a recovery of 89.6% ± 2.2%.

Zeta potential analysis

Figure 4 illustrates the zeta potential of Py and CPy both before and after treatment with the biocollector at natural pH in both distilled water (Dw) and Sw. In Dw (Fig. 4a), the zeta potential of Py conditioned under an open atmosphere exhibits a negative surface potential until pH 4, after which the zeta potential becomes increasingly positive, reaching its highest value at pH 8 with 4.9 ± 0.05 mV. In the case of CPy, the zeta potential at pH 2 was 4.73 ± 0.02 mV, becoming more negative as pH increases. Conversely, the zeta potential of the bacteria alone ranges from −7.93 ± 0.05 at pH 2, remaining relatively constant from pH 4 to pH 10 within the range of −24.06 ± 0.1 to −22.7 ± 0.02 mV. Furthermore, the interaction of the biocollector with Py and CPy induces changes in their zeta potential, rendering them more negative and akin to the zeta potential of the biocollector alone.

In Sw conditions (Fig. 4b), the zeta potential of Py conditioned under an open atmosphere exhibits a negative surface potential across varying pH levels. However, at pH 10, the potential becomes positive. In the case of CPy, throughout all analyzed pH levels, the zeta potential is negative, albeit to a lesser extent than that of the bacteria alone. Moreover, the interaction of both minerals with the biocollector induces a behavior similar to that observed in Dw, rendering the zeta potential more negative.

FTIR measurements

Figure 5 shows the FTIR spectra of the *B. subtilis* LN8B treated with Sw and Dw. In both spectra, the presence of the proteins was identified through the amide peaks along the spectra. Thus, the characteristic absorption bands of the protein were identified at 3322 cm^{-1} attributed to the symmetric stretching vibration of NH_2. The band at 3083 cm^{-1} can be assigned to NH_3 and the band at 2929 cm^{-1} can be assigned to C–H stretching of CH_2 and CH_3 groups. The band at 1650 cm^{-1} is characteristic of the C=O stretching of Amide I in the protein. The band at 1550 cm^{-1} is characteristic of NH bending and CN stretching vibrations of the Amide II in the protein. The band at 1454 cm^{-1} is attributed to the asymmetric bending vibration of CH_3. The band at 1400 cm^{-1} is associated with the symmetric stretching of COO^- and the band at 1334 cm^{-1} can be assigned to the bending vibration of CH. The band at 1245 cm^{-1} is attributed to the bending vibration of COH. Finally, the band at 1060 cm^{-1} can be assigned to the rocking of the CH_3. It is worth mentioning that the water type does not influence the speciation of bacteria, because it identified the same adsorption bands in both spectra (Le Gal et al. 1991, Garcia et al. 2008, Alvarez-Ordóñez et al. 2011, Yang et al. 2013, Hong et al. 2018).

Figure 6 shows the FTIR spectra of the minerals (CPy and Py) before and after interaction with the biocollector. The absorption of bacteria on the CPy surface was evidenced in the range between 1650 and 1060 cm^{-1} (Fig. 6a). Strong bands of Amide I and Amide II were identified on the CPy surface. Also, a broad band was identified at 3322 cm^{-1}, attributed to NH_2. Therefore, these bands enable to identify the absorption of the bacteria on the CPy surface. Regarding the Py (Fig. 6b), the same behavior and bands were absorbed onto the Py surface, except for the band located at 3322 cm^{-1}, which was absent in both cases when the Py was treated with Sw and Dw. These results enable us to identify bacteria absorption on the Py surface. Table 5 summarizes all the peaks indexed in the spectra.

Discussions

The Atacama Desert in northern Chile is considered one of the driest territories on Earth, with high solar insolation, rich in mineral resources, and a previously unexpected microbial richness adapted to extreme environmental factors (Gómez-

Downloaded from https://academic.oup.com/jambio/article/135/1/lxad313/7485925 by Universidad de Antofagasta user on 26 January 2026

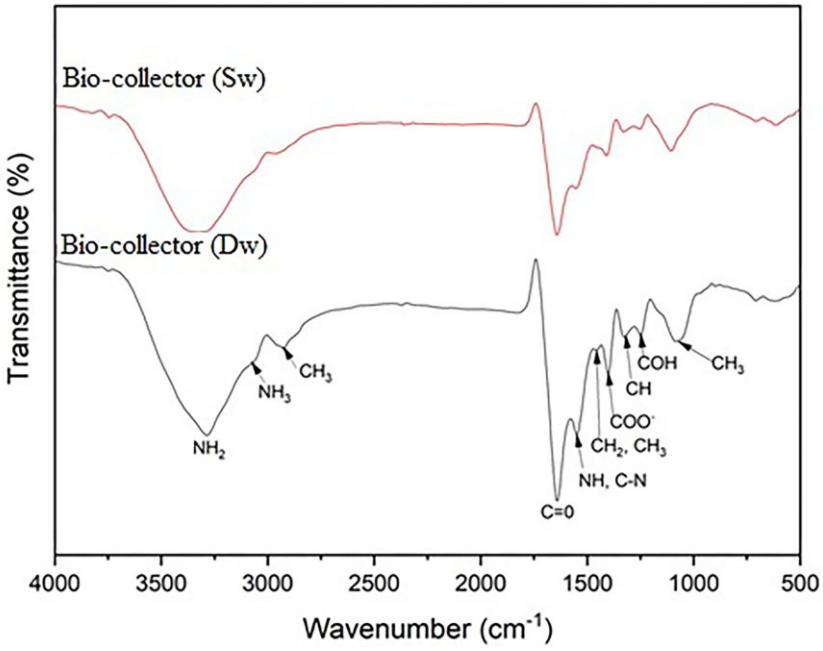


Figure 5. FTIR spectra of the *B. subtilis* LN8B (biocollector) in Sw and Dw.

Silva 2018, Gómez-Silva and Batista-García 2022). Because *B. subtilis* LN8B is able to grow in Sw, these results provide a reasonable alternative for using Sw in the biomass-based industries, reducing their dependency on freshwater resources, particularly in northern Chile. *Bacillus subtilis* species are present in various environments; however, the interesting thing about the strain used in this study is its halotolerance. Halotolerant microorganisms as sources of organic compounds are gaining attention, and most reports on biorefinery inform the use of Sw for the production of microalgal biomass (Gómez-Silva 2018, Gómez-Silva and Batista-García 2022). Also, the production of halotolerant cellulases has been reported on marine bacterial strains (*B. oceanisediminis*, *Brevibacterium halotolerans*, and *Psychrobacter celer*) (Pugazhendhi et al. 2020); comparatively, the best biomass saccharifying performance was obtained with *Br. halotolerans*, a promising candidate for cellulase production for the Sw-based biofuel industry.

Since resistance/susceptibility to antibiotics is particularly important for the use of microorganisms, *B. subtilis* LN8B is susceptible to 23 from 25 antibiotics studied; accordingly, it is possible to propose that is not a microorganism of clinical or environmental concern (Sales et al. 2017). Indeed, *B. subtilis* LN8B was resistance to cefepime, a commonly used antibiotic normally utilized to control Gram-negative bacteria, which could be explained because *B. subtilis* is a Gram-positive bacterium (Gupta et al. 2023). In addition, *B. subtilis* LN8B was also slightly resistance to fosfomicyn, which is a broad-spectrum antibiotic. Therefore, our results support the use of the biocollector and its derived products for many industrial uses, as well as probiotics and biocontrol processes (Arnaouteli et al. 2021).

The bioflotation results presented in the "Bioflotation tests" section support the use of *B. subtilis* LN8B as biocollector. Also, the results obtained from the FTIR, support the zeta potential findings, since it was identified that the majority of species present on the bacteria surface was hydrophobic. Specifically, the negative potential for Py in Dw could be due to the sulfur-rich surface and iron deficiency, demonstrating a nonoxidized surface (Paredes et al. 2019). Then, two isoelectric points were identified, one at pH 6 and the other at pH 8.5, in this pH range, the zeta potential was positive. This could be attributed to the oxidation of Py due to the formation of ferric oxyhydroxides on the pyrite surface (Fuerstenau et al. 1990, Valdivieso et al. 2005, Paredes et al. 2019). Then, at pH 10, the zeta potential became negative; this could be due to the formation of simple iron hydroxide (goethite) on pyrite surface. This is an intermediate oxidation product with a negative zeta potential for alkaline pH surface (Kosmulski et al. 2003, Paredes et al. 2019).

The zeta potential of CPy treated under an open atmosphere remains negative along pH, demonstrating the nonoxidized surface. Then, the zeta potential of the biocollector remains negative along the pH studied. When the CPy and Py interact with the biocollector, the zeta potential for both minerals becomes more negative along pH due to biocollector adsorption on mineral surfaces through electrostatic attraction between particles and bacteria species (Yang et al. 2013). This demonstrated the biocollector effect on increasing the hydrophobicity of mineral surfaces in Dw. The analysis of zeta potential in Sw indicates that pyrite conditioned under an open atmosphere possesses a negative surface potential from the pH 2 to pH 8. This could be due to the presence of bivalent cations such as Ca^{2+} and Mg^{2+} in Sw, which neutralize the negative charges on nonoxide and oxide sites on the pyrite surface, forming a coating of cations and therefore avoiding pyrite oxidation (Paredes et al. 2019, Xue et al. 2022, Texeira et al. 2023). However, a noteworthy observation is that at a pH of 10, the potential undergoes a shift and becomes positive. This could be due to the formation of $Mg(OH)_2$ solid species onto the Py surface. It is well known that this divalent salt in Sw is formed at pH values >9.5 (Li et al. 2018). On the other hand, the zeta potential of CPy treated under an open atmosphere remains negative along pH, demonstrating the nonoxidized surface. Then, the zeta potential of the biocollector remains negative along the pH studied. This demonstrates that,

Downloaded from https://academic.oup.com/jambio/article/135/1/lxad313/7485925 by Universidad de Antofagasta user on 26 January 2026

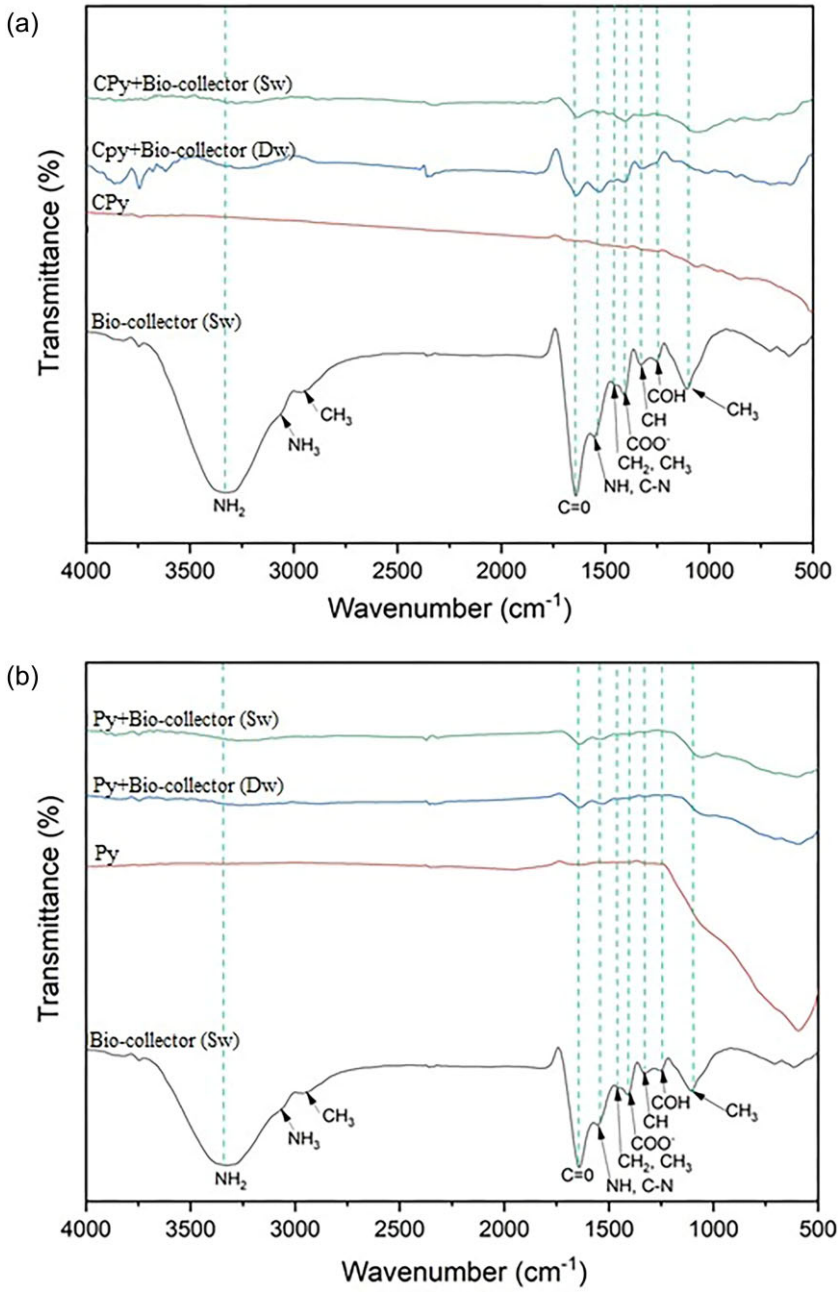


Figure 6. FTIR spectra of CPy (a) and Py (b) before and after treatment with *B. subtilis* LN8B at natural pH in Sw and Dw.

Table 5. Vibrational frequencies of *B. subtilis* LN8B.

Frequencies (cm^{-1})	Assignment (*)	References
3322	δ_s (NH_2)	Le Gal et al. (1991), Garcia et al. (2008), Alvarez-Ordóñez et al. (2011), Yang et al. (2013), Hong et al. (2018)
3083	NH_3	
2929	*u* (CH)	
1650	*u* (C=O)	
1550	δ (N–H) + *u* (C–N)	
1454	δ_{as} (CH_3)	
1400	u_s (COO^-)	
1334	δ (CH)	
1245	δ (COH)	
1060	ρ (CH_3)	

(*) *u*, stretching; ρ, rocking; δ, bending; s, symmetric; and as, asymmetric.

Downloaded from https://academic.oup.com/jambio/article/135/1/lxad313/7485925 by Universidad de Antofagasta user on 26 January 2026

despite the complex composition of Sw, including ions such as chloride, sulfate, magnesium, calcium, and carbonate, among others, which may potentially influence the flotation process, there are no precipitated compounds formed between bacteria and Sw. This allows the bacteria to exhibit the same behavior as described in Dw. Then, when the CPy and Py interact with the biocollector, the zeta potential for both minerals becomes more negative along pH due to biocollector adsorption on mineral surfaces through electrostatic attraction between particles and bacteria species. This demonstrates once again the effect of the biocollector on increasing the hydrophobicity of mineral surfaces (Li et al. 2019, Arancibia-Bravo et al. 2020, 2021). Therefore, the biocollector could be used as a collector for CPy and Py flotation either in Dw or Sw. On the other hand, the FTIR spectra of the *B. subtilis* LN8B treated with Sw and Dw confirmed the presence of the proteins through the amide peaks along the spectra, which justifies the bacteria hydrophobicity. Therefore, it is likely to use this bacterial strain as a collector in the flotation of Py and CPy. It was also determined the type of amino acid that corresponds to the strong band identified at 1650 cm^{-1}; this can be attributed to the α-Alanine. Alanine is one of the amino acids present in bacteria (Ttilio et al. 1997). The adsorption bands at 1454, 1334, 1245, and 1060 cm^{-1} were also attributed to the α-Alanine amino acid (Ttilio et al. 1997). In the case of FTIR spectra of the minerals (CPy and Py) before and after interaction with the biocollector, it was evidenced that the type of water does not influence how *B. subtilis* is adsorbed on the mineral's surface. Therefore, the active hydrophobic species on the mineral's surface responsible for CPy and Py flotation are leading by Amide I and Amide II present in the protein. These results enable us to conclude that it is likely to use the *B. subtilis* LN8B as a biocollector for the flotation of CPy and Py at natural pH using Sw and Dw.

Our study agrees with numerous studies suggesting that some bioreagents' hydrophobic nature is influenced by its protein content, while its hydrophilic properties are associated with its polysaccharide concentration (Merma et al. 2013, Olivera et al. 2017). This agrees with what is described by Sarvamangala et al. (2013), which studied the microbially induced Py removal from galena using *B. subtilis*. Py was depressed by the exopolysaccharides that were produced, whereas galena surfaces were rendered hydrophobic by the extracellular proteins that were generated. On the other hand, Abedi Ashkavandi et al. (2022) studied the influence of the *B. licheniformis* as biocollector for selective flotation of barite ($BaSO_4$) from quartz (SiO_2). Barite was recovered up to 87% (at pH = 3) in sole-mineral flotation experiments, and flotation of the mixed sample, also, proved a successful selective separation of barite (76% recovery) from quartz at the biocollector dosage of 6.55×10^3 cells ml^{-1}. However, not all proteins act as collectors, e.g. Yehia et al. (2017, 2019) have shown that enzymes such as cellulase and amylase have a natural depressant effect property, which may improve the flotation of apatite iron oxide and phosphate-dolomite complexes. Therefore, proteins or enzymes exhibit high surface activity due to their amphiphilic structure, i.e. they possess both hydrophilic and hydrophobic side chain functional groups (Ammar et al. 2022).

It is worth mentioning that this work looks to find alternative biocollectors to conduct the desulfurization process of sulfide minerals and produce tailings with low content of sulfide species framed in the concept of cleaner production. Therefore, the fact that the *B. subtilis* LN8B could be used as a bulk collector in the flotation process gives us alternatives to future mineral processing practices to prevent AMD from tailings.

Conclusions

Bacillus subtilis LN8B exhibited the remarkable ability to thrive both in Sw and Dw, highlighting its adaptability and versatility for various applications. Sw as a resource for biomass-based industries presents a significant opportunity to reduce freshwater dependency, particularly in regions like northern Chile.

The susceptibility profile of *B. subtilis* LN8B to antibiotics, with susceptibility to 23 out of 25 tested antibiotics, underscores its safety and suitability for use in industrial and environmental contexts. This suggests that the strain poses minimal clinical or environmental concerns, further enhancing its attractiveness as a biocollector.

The study's experimental results in Sw revealed compelling advantages. Without the presence of microorganisms, sulfide mineral recovery rates, specifically for Py and CPy, were low, standing at ~39.3% ± 7.7% and 41.1% ± 5.8%, respectively. However, introducing *B. subtilis* LN8B as a biocollector substantially enhanced Py recovery to ~72.8% ± 4.9% and CPy recovery to an impressive 84.6% ± 1.5%. For Py, these gains were further amplified when a frother (MIBC) was incorporated into the system, culminating in recovery reaching 89.4% ± 3.6%.

Fundamental insight into the physicochemical interactions revealed that when CPy and Py interacted with the biocollector, the zeta potential for both minerals became more negative with increasing pH. This was attributed to the adsorption of the biocollector onto mineral surfaces through electrostatic attraction between the particles and bacterial species. Hence, the pivotal hydrophobic entities residing on the mineral's surface, which play a crucial role in the flotation of CPy and Py, are primarily represented by the presence of Amide I and Amide II within the protein.

Finally, these results together indicate the potential utility of *B. subtilis* LN8B as a biocollector for CPy and Py flotation. This work aligns with the objective of finding alternative reagents, such as biocollectors, to facilitate the desulfurization process of sulfide minerals. However, additional experiments are needed to corroborate these results as laboratory-scale flotation tests with waste rock minerals and complementary analyses of the interaction of the biocollector with minerals such as Field-Emission Scanning Electron Microscopy (FE-SEM) and X-ray photoelectron spectroscopy (XPS).

Acknowledgments

The authors would like to express their gratitude to Dr. Mariella Rivas for providing the bacterial strain for the use in the present manuscript.

Supplementary data

Supplementary data is available at *JAMBIO Journal* online.

Conflict of interest: None declared.

Downloaded from https://academic.oup.com/jambio/article/135/1/lxad313/7485925 by Universidad de Antofagasta user on 26 January 2026

Funding

The authors thank the financial support from the Agencia Nacional de Investigación y Desarrollo-ANID through the programs Fondecyt Postdoctoral project # 3210675 and PIA program ANID/ACT210027.

Author contributions

Dayana Arias (Conceptualization, Formal analysis, Funding acquisition, Investigation, Writing – review & editing), Manuel Saldaña (Conceptualization, Writing – review & editing), Yesica L. Botero (Formal analysis, Investigation, Writing – original draft), Francisco Dinamarca (Investigation, Methodology), Bernardo Paredes (Investigation, Methodology), Camila Salazar-Ardiles (Investigation, Methodology), David C. Andrade (Resources, Writing – review & editing), Luis A. Cisternas (Resources, Writing – review & editing), Jorge Carrasco (Investigation), Carlos Santos (Investigation), Cristina Dorador (Resources, Writing – review & editing), and Benito Gómez-Silva (Resources, Writing – review & editing)

Data availability

The authors confirm that the data supporting the findings of this study are available within the article.

References

Abedi Ashkavandi R, Azimi E, Hosseini MR. *Bacillus licheniformis* a potential bio-collector for Barite–Quartz selective separation. *Miner Eng* 2022;**175**:107285. https://doi.org/10.1016/j.mineng.2021.107285.

Ait-Khouia Y, Benzaazoua M, Demers I. Environmental desulfurization of mine wastes using various mineral processing techniques: recent advances and opportunities. *Miner Eng* 2021;**174**:1–18. https://doi.org/10.1016/j.mineng.2021.107225.

Aksoy DÖ, Özdemir S, Aytar Çelik P *et al*. Fusion of the microbial world into the flotation process. *Miner Process Extr Metall Rev* 2022;**00**:1–15.

Alvarez-Ordóñez A, Mouwen DJM, López M *et al*. Fourier transform infrared spectroscopy as a tool to characterize molecular composition and stress response in foodborne pathogenic bacteria. *J Microbiol Methods* 2011;**84**:369–78. https://doi.org/10.1016/j.mimet.2011.01.009.

Ammar M, El-Halim SA, Sharada H *et al*. Study on the interactions of two models of enzymes as eco-friendly depressants in flotation separation of apatite from hematite. *Appl Surf Sci* 2022;**601**:1–12. https://doi.org/10.1016/j.apsusc.2022.154223.

Arancibia-Bravo M, Lucay F, Sepulveda F *et al*. On the use of Na_2SO_3 as a pyrite depressant in saline systems and the presence of kaolinite. *Physicochem Probl Miner Process* 2021;**57**:168–79. https://doi.org/10.37190/ppmp/139511.

Arancibia-Bravo MP, López-Valdivieso A, Flores LF *et al*. Effects of potassium propyl xanthate collector and sodium sulfite depressant on the floatability of chalcopyrite in seawater and KCl solutions. *Minerals* 2020;**10**:991. https://doi.org/10.3390/min10110991.

Arancibia-Bravo MP, Lucay FA, López J *et al*. Modeling the effect of air flow, impeller speed, frother dosages, and salt concentrations on the bubbles size using response surface methodology. *Miner Eng* 2019;**132**:142–8. https://doi.org/10.1016/j.mineng.2018.12.001.

Arias D, Cisternas LA, Miranda C *et al*. Bioprospecting of ureolytic bacteria from Laguna Salada for biomineralization applications. *Front Bioeng Biotechnol* 2019;**6**:1–13. https://doi.org/10.3389/fbioe.2018.00209.

Arias D, Salazar-Ardiles C, Andrade DC *et al*. The microbial world in copper sulfide flotation plants (CSFP): novel insights into bacterial communities and their application as potential pyrite bioreagents. *Environ Res* 2023;**218**:1–12. https://doi.org/10.1016/j.envres.2022.114904.

Arnaouteli S, Bamford NC, Stanley-Wall NR *et al*. Bacillus subtilis biofilm formation and social interactions. *Nat Rev Micro* 2021;**19**:600–14. https://doi.org/10.1038/s41579-021-00540-9.

Benzaazoua M, Bouzahzah H, Taha Y *et al*. Integrated environmental management of pyrrhotite tailings at Raglan Mine: part 1 challenges of desulphurization process and reactivity prediction. *J Clean Prod* 2017;**162**:86–95. https://doi.org/10.1016/j.jclepro.2017.05.161.

Benzaazoua M, Bussière B, Kongolo M *et al*. Environmental desulphurization of four Canadian mine tailings using froth flotation. *Int J Miner Process* 2000;**60**:57–74. https://doi.org/10.1016/S0301-7516(00)00006-5.

Botero YL, Canales-Mahuzier A, Serna-Guerrero R *et al*. Physical–chemical study of IPETC and PAX collector's adsorption on covellite surface. *Appl Surf Sci* 2022;**602**:1–16. https://doi.org/10.1016/j.apsusc.2022.154232.

Castro S, Miranda C, Toledo P *et al*. Effect of frothers on bubble coalescence and foaming in electrolyte solutions and seawater. *Int J Miner Process* 2013;**124**:8–14. https://doi.org/10.1016/j.minpro.2013.07.002.

Cisternas LA, Gálvez ED. The use of seawater in mining. *Miner Process Extr Metall Rev* 2018;**39**:18–33. https://doi.org/10.1080/08827508.2017.1389729.

Dwyer R, Bruckard WJ, Rea S *et al*. Bioflotation and bioflocculation review: microorganisms relevant for mineral beneficiation. *Miner Process Extr Metall Trans Inst Min Metall* 2012;**121**:65–71.

Elshkaki A, Graedel TE, Ciacci L *et al*. Copper demand, supply, and associated energy use to 2050. *Glob Environ Chang* 2016;**39**:305–15. https://doi.org/10.1016/j.gloenvcha.2016.06.006.

Fuerstenau MC, Misra M, Palmer BR. Xanthate adsorption on selected sulfides in the virtual absence and presence of oxygen, Part 2 *International Journal of Mineral Processing*, 1990;**29**: no 1-2, p. 111–9.

Garcia AR, de Barros RB, Lourenço JP *et al*. The infrared spectrum of solid L-alanine: influence of pH-induced structural changes. *J Phys Chem A* 2008;**112**:8280–7. https://doi.org/10.1021/jp802170n.

Gómez-Silva B, Batista-García RA. The Atacama desert: a biodiversity hotspot and not just a mineral-rich region. *Front Microbiol* 2022;**13**:1–5. https://doi.org/10.3389/fmicb.2022.812842.

Gómez-Silva B. Lithobiontic life: "Atacama rocks are well and alive." *Antonie Van Leeuwenhoek, Int J Gen Mol Microbiol* 2018;**111**:1333–43. https://doi.org/10.1007/s10482-018-1033-9.

Gupta L, Saxena K, Goyal R. Antibiotic challenges and review of appropriate uses in intensive care unit. *J Indian Coll Anaesth* 2023;**2**:7–17.

Hong Z-N, Jiang J, Li J-Y *et al*. Preferential adhesion of surface groups of *Bacillus subtilis* on gibbsite at different ionic strengths and pHs revealed by ATR-FTIR spectroscopy. *Colloids Surf B Biointerfaces* 2018;**165**:83–91. https://doi.org/10.1016/j.colsurfb.2018.02.020.

Jeldres RI, Forbes L, Cisternas LA. Effect of seawater on sulfide ore flotation: a review. *Miner Process Extr Metall Rev* 2016;**37**:369–84. https://doi.org/10.1080/08827508.2016.1218871.

Kosmulski, M., Maczka, E., Jartych, E.,Synthesis and characterization of goethite and goethite–hematite composite: experimental study and literature survey 2003 **103** 57–76.

Le Gal J-M, Manfait M, Theophanides T. Applications of FTIR spectroscopy studies of cells and bacteria. *J Mol Struct* 1991;**242**:397–407. https://doi.org/10.1016/0022-2860(91)87150-G.

Li W, Li Y, Xiao Q *et al*. The influencing mechanisms of sodium hexametaphosphate on chalcopyrite flotation in the presence of MgCl2 and CaCl2. *Minerals* 2018;**8**:150. https://doi.org/10.3390/min8040150.

Li Y, Zhu H, Li W *et al*. A fundamental study of chalcopyrite flotation in sea water using sodium silicate. *Miner Eng* 2019;**139**:105862. https://doi.org/10.1016/j.mineng.2019.105862.

Downloaded from https://academic.oup.com/jambio/article/135/1/lxad313/7485925 by Universidad de Antofagasta user on 26 January 2026

Martínez GM, Pire C, Martínez-Espinosa RM. Hypersaline environments as natural sources of microbes with potential applications in biotechnology: the case of solar evaporation systems to produce salt in Alicante County (Spain). *Curr Res Microb Sci* 2022;**3**:1–13. https://doi.org/10.1016/j.crmicr.2022.100136.

Merma AG, Torem ML, Morán JJV *et al*. On the fundamental aspects of apatite and quartz flotation using a Gram positive strain as a bioreagent. *Miner Eng* 2013;**48**:61–7. https://doi.org/10.1016/j.mineng.2012.10.018.

Nadeif A, Taha Y, Bouzahzah H *et al*. Desulfurization of the old tailings at the Au-Ag-Cu Tiouit Mine (Anti-Atlas Morocco). *Minerals* 2019;**9**:401. https://doi.org/10.3390/min9070401.

Olivera CAC, Merma AG, Puelles JGS *et al*. On the fundamentals aspects of hematite bioflotation using a Gram positive strain. *Miner Eng* 2017;**106**:55–63. https://doi.org/10.1016/j.mineng.2016.10.017.

Oulkhir A, Lyamlouli K, Danouche M *et al*. A critical review on natural surfactants and their potential for sustainable mineral flotation. *Rev Environ Sci Biotechnol* 2023;**22**:105–31. https://doi.org/10.1007/s11157-022-09639-8.

Paredes A, Acuña SM, Gutiérrez L *et al*. Zeta potential of pyrite particles in concentrated solutions of monovalent seawater electrolytes and amyl xanthate. *Minerals* 2019;**9**:584. https://doi.org/10.3390/min9100584.

Pugazhendhi A, Nagappan S, Bhosale RR *et al*. Various potential techniques to reduce the water footprint of microalgal biomass production for biofuel—a review. *Sci Total Environ* 2020;**749**:1–13. https://doi.org/10.1016/j.scitotenv.2020.142218.

Rao F, Lázaro I, Ibarra LA. Solution chemistry of sulphide mineral flotation in recycled water and sea water: a review. *Miner Process Extr Metall* 2017;**126**:139–45. https://doi.org/10.1080/03719553.2016.1192794.

Rao KH, Vilinska A, Chernyshova IV. Minerals bioprocessing: R & D needs in mineral biobeneficiation. *Hydrometallurgy* 2010;**104**:465–70.

Sales DL, Morais-Braga MFB, dos Santos ATL *et al*. Antibacterial, modulatory activity of antibiotics and toxicity from Rhinella jimi (Stevaux, 2002) (Anura: Bufonidae) glandular secretions. *Biomed Pharmacother* 2017;**92**:554–61. https://doi.org/10.1016/j.biopha.2017.05.098.

Sarvamangala H, Natarajan KA, Girisha ST. Microbially-induced pyrite removal from galena using *Bacillus subtilis*. *Int J Miner Process* 2013;**120**:15–21. https://doi.org/10.1016/j.minpro.2013.02.005.

Shen Y, Nagaraj DR, Farinato R *et al*. Study of xanthate decomposition in aqueous solutions. *Miner Eng* 2016;**93**:10–5.

Skandrani A, Demers I, Kongolo M. Desulfurization of aged gold-bearing mine tailings. *Miner Eng* 2019;**138**:195–203. https://doi.org/10.1016/j.mineng.2019.04.037.

Suyantara GPW, Hirajima T, Miki H *et al*. Floatability of molybdenite and chalcopyrite in artificial seawater. *Miner Eng* 2018;**115**:117–30. https://doi.org/10.1016/j.mineng.2017.10.004.

TEXEIRA L, Impact of the use of seawater on acid mine drainage from mining wastes. *Journal of Cleaner Production*, 2023;**383**:135516. https://www.sciencedirect.com/science/article/pii/S0959652622050909?casa_token=ooiiFFbd6vcAAAAA:Eurs-VPMTIqjaSjINngnWei_s8-YW0-NQOsaL8bb2deFJMBi3UhxkjbbZH-I8S1__98rB6V_hrrT.

Ttilio M, Rosadoa S, Leonor M *et al*. Vibrational spectra (FT-IR, Raman and MI-IR) of α-and β-alanine. *J Mol Struct* 1997;**410**:343–8.

Valdivieso A, López AA, Sánchez S. On the cathodic reaction coupled with the oxidation of xanthates at the pyrite/aqueous solution interface. *International Journal of Mineral Processing*, 2005;**77**:154–64.

Wills BA, Napier-Munn TJ. *Wills' Mineral Processing Technology*. Burlington, MA: Elsevier, 2016.

Xue J, Fuchida S, Ishida S. Insight on exogenous calcium/magnesium in weakening pyrite floatability with prolonged pre-oxidation: localized and concomitant secondary minerals and their depression characteristics. *Minerals* 2022;**12**:1–16.

Yang H, Tang Q, Wang C *et al*. Flocculation and flotation response of *Rhodococcus erythropolis* to pure minerals in hematite ores. *Miner Eng* 2013;**45**:67–72. https://doi.org/10.1016/j.mineng.2013.01.005.

Yehia A, Khalek MA, Ammar M. Cellulase as a new phosphate depressant in dolomite-phosphate flotation. *Physicochem Probl Miner Process* 2017;**53**:1092–104.

Yehia A, Yassin KE, Amar M. Upgrading of phosphate fines by fatty acid flotation using amylase enzyme as a surface modifier. *Min Metall Explor* 2019;**36**:949–55.

Yin J, Chen JC, Wu Q *et al*. Halophiles, coming stars for industrial biotechnology. *Biotechnol Adv* 2015;**33**:1433–42. https://doi.org/10.1016/j.biotechadv.2014.10.008.

Received 20 November 2023; **revised** 12 December 2023; **accepted** 19 December 2023
© The Author(s) 2023. Published by Oxford University Press on behalf of Applied Microbiology International. All rights reserved. For permissions, please e-mail: journals.permissions@oup.com

Downloaded from https://academic.oup.com/jambio/article/135/1/lxad313/7485925 by Universidad de Antofagasta user on 26 January 2026